

Communication

# Kerr-Nonlinearity-Triggered Nonclassicality of Magnons in a Photon-Magnon Coupling System

Xi Jiang <sup>1</sup>, Shiqing Tang <sup>1,2,\*</sup> and Songsong Li <sup>3</sup>

- <sup>1</sup> College of Physics and Electronic Engineering, Hengyang Normal University, Hengyang 421002, China  
<sup>2</sup> Key Laboratory of Low-Dimensional Quantum Structures and Quantum Control of Ministry of Education, Hunan Normal University, Changsha 410081, China  
<sup>3</sup> College of Physics and Electronic Information, Nanchang Normal University, Nanchang 330032, China  
\* Correspondence: sqtang@hynu.edu.cn

**Abstract:** Hybrid quantum systems have attracted much attention due to the fact that they combine the advantages of different physical subsystems. Cavity QED (cavity quantum electrodynamics) with magnons is a hybrid quantum systems that combines a YIG (Yttrium Iron Garnet) sphere and a 3D (three-dimensional) rectangular microwave cavity. Based on this hybrid photon-magnon system, we obtain an approximate analytic solution by the RWA (rotating wave approximation) with an ingenious transformation. After skillfully diagonalizing the Hamiltonian, we show that the Kerr-nonlinearity interactions could yield a negativity value of the Wigner function, periodic quadrature squeezing effects, antibunching property, and field nonclassicality in the magnon. Our work may stimulate the study of nonclassicality of photon-magnon coupling systems and its potential applications in quantum information processing.

**Keywords:** microwave cavity; photon; magnon; nonclassicality



**Citation:** Jiang, X.; Tang, S.; Li, S. Kerr-Nonlinearity-Triggered Nonclassicality of Magnons in a Photon-Magnon Coupling System. *Photonics* **2022**, *9*, 681. <https://doi.org/10.3390/photonics9100681>

Received: 2 September 2022

Accepted: 17 September 2022

Published: 21 September 2022

**Publisher's Note:** MDPI stays neutral with regard to jurisdictional claims in published maps and institutional affiliations.



**Copyright:** © 2022 by the authors. Licensee MDPI, Basel, Switzerland. This article is an open access article distributed under the terms and conditions of the Creative Commons Attribution (CC BY) license (<https://creativecommons.org/licenses/by/4.0/>).

## 1. Introduction

As we all know, scientists can manipulate various systems at the single quantum level. However, no single type of system can meet all the requirements of quantum information technology. For example, superconducting is recognized as the most competitive solution for scalable solid-state quantum computing, and it is also known to be the nonlinear device with the best performance in the microwave frequency band and ultralow temperature region, but its decoherence time is currently lower than that of natural atoms or ions by three orders of magnitude. Therefore, researchers naturally conceived of utilizing the advantages of solid-state systems, such as microwave resonators, magnon qubits, nanomechanical oscillators and superconducting qubits, to build solid-state hybrid quantum systems with different functions to realize the optimized quantum information processing scheme, which can be explored as a new physical realization method for new quantum computing and meet the development needs of quantum information technology. The purpose of mixing and hybridization is to naturally take advantage of their own strengths and to perform their own duties and functions to achieve more complex and complete information processing, information storage and information transmission functions. In recent years, hybrid quantum systems have attracted much attention due to the fact that they combine the advantages of different physical subsystems [1,2]. Over the past few years, scientists have theoretically proposed [3,4] a hybrid system based on the formation of spin ensemble-coupled microwave cavity modes in single-crystal YIG samples, and obtained experimental verification [5,6]. Unlike spin ensembles in paramagnetic materials with a lower density (such as nitrogen-vacancy color centers in diamonds [7]), spin ensembles in ferromagnetic YIG materials have higher spin densities ( $\sim 2.1 \times 10^{22} \text{ cm}^{-3}$ ) and a low dissipation rate, and can be fully polarized below the Curie temperature ( $\sim 559 \text{ K}$ ) [8]. Experimentally, a strong coupling between spin ensembles and microwave cavity modes has been achieved

in YIG samples [9], which is extremely difficult for spin ensembles in paramagnetic materials. Many exotic phenomena can be observed in cavity-magnon systems, such as cavity spin-wave excitons [10,11], super strong coupling [12,13], mutual conversion between microwave photons and optical photons [13], synchronous spin-photon coupling [14,15], spin-wave dark mode [16], cavity spintronics [17], optical manipulation of cavity spin-wave systems [18], interlayer strong coupling of spin-waves [19], dynamical behavior of collective polaritons [20] and non-Hermitian physics. In addition, spin-wave quanta can also form a strong coupling with other quantum systems, such as superconducting qubits [21], phonons and optical whispering gallery cavities [22]. The above studies all approximate the wave color mode in the YIG sample as a linear harmonic oscillator. However, this approximation only holds under the low-power drive of cavity spin-wave systems. Under high-power driving, the nonlinear effects of the spin-wave mode in YIG will be obviously manifested, such as the bistable effect [23] and the chaotic effect [24].

Enlightened by the above-mentioned works about magnons, we construct a theoretical model of the hybrid quantum structure, which contains a YIG sphere coupling with a 3D microwave cavity, to explore nonclassical behaviors of the magnons' Kerr interaction. In this photon-magnon system, we diagonalize the Hamiltonian of the cavity spin-wave hybrid system with an ingenious transformation. Resorting to the concept of magnon coherent states, we investigate the quantum dynamics of the magnons and find that magnon Kerr nonlinearity can trigger nonclassical properties, such as negativity value of the Wigner function, quadrature squeezing effects, antibunching property and field nonclassicality in the magnon. These hybrid quantum systems may be useful in the preparation of magnon nonclassical states and the realization of a single magnon source.

## 2. The Model

Considering a cavity-magnonic system consisting of a cavity mode and a Kittel mode of the magnon, the magnetic dipole-dipole interaction of the Kittel mode with cavity photons could yield a nonlinear model. The Hamiltonian of this cavity-magnonic system can be written as (assume  $\hbar = 1$ )

$$H = H_c + H_m + H_{int} \tag{1}$$

where  $H_c$  in Equation (1) is the Hamiltonian of the cavity mode, i.e.,

$$H_c = \omega_c a^\dagger a \tag{2}$$

The corresponding creation and annihilation operators for cavity mode  $c$  (with frequency  $\omega_c$ ) are  $a^\dagger$  and  $a$ , respectively. The interaction between the magnons and photons in the system is introduced by a YIG material sphere placed in the cavity. For the YIG sphere which is uniformly magnetized, its Hamiltonian can be written as two parts [25–28], i.e., the Zeeman energy and the magneto crystalline anisotropic energy [29]:

$$H_m = - \int M_m \cdot B_0 d\tau - \frac{\mu_0}{2} \int M_m \cdot H_m^{an} d\tau \tag{3}$$

Here,  $B_0$  represents the applied static magnetic field, and  $\tau$  and  $\mu_0$  are the volume and vacuum permeability of the YIG sphere, respectively.  $M_m$  is the magnetization of the Kittel mode in the YIG sphere, and  $B_0 = B_0 e_z$  is the magnetic field along the  $z$  direction.  $H_m^{an}$  represents the energy caused by the anisotropy of the magnetic medium inside the YIG sphere. In case the crystal axis [100] of the YIG sphere is also along the  $z$  direction, the anisotropic field  $H_m^{an}$  is [30–39]  $H_m^{an} = \frac{2\hbar\gamma_g S_z^m K_{an}^m}{\mu_0 M^2 \tau} e_z$ , where  $K_{an}^m$  is the dominant first-order anisotropic coefficient and  $M$  is the saturation magnetization. After the Holstein-Primakoff transformation, the simplified Hamiltonian with respect to the magnon becomes

$$H_m = \omega_m m^\dagger m + K (m^\dagger m)^2 \tag{4}$$

where symbol  $m^\dagger(m)$  represents the magnon creation (annihilation) operator of cavity spin-wave quanta, and the corresponding frequency is  $\omega_m = \gamma_g B_0 - \frac{2\hbar\gamma_g^2 K_{am}^m S_m}{M^2 V_{YIG}}$ .  $\gamma_g$  is the gyromagnetic ration. The final term  $K(m^\dagger m)^2$  characterizes the Kerr effect of the magnons. The coefficient  $K$  can be calculated by  $K = -\frac{\hbar\gamma_g^2 K_{am}^m}{M^2 \tau}$ , which represents the intensity of the magnon Kerr nonlinearity. The magnon-photon interaction Hamiltonian is  $H_{int} = -\mu_0 \int M_m \cdot B_a d\tau$ , where the magnetic field  $B_a = -(\hbar\omega_c / \mu_0 V_c)^{1/2} (\hat{a}^\dagger + \hat{a}) e_x$  of the cavity mode is polarized in the  $x$  direction, with  $V_c$  being the volume of the cavity. Under the RWA in the second quantization, the interaction Hamiltonian can be simplified as

$$H_{int} = g(a^\dagger m + am^\dagger) \tag{5}$$

Then, the total effective Hamiltonian of the photon-magnon system [30–39] is

$$H_{eff} = \omega_c a^\dagger a + \omega_m m^\dagger m + K(m^\dagger m)^2 + g(a^\dagger m + am^\dagger) \tag{6}$$

In order to diagonalize the Hamiltonian, we use a new pair of bosonic operators  $A_1$  and  $A_2$  [40–42], and its expressions are:

$$a(t) = \frac{1}{\sqrt{2}} [A_1(t)e^{i2gt} - iA_2(t)e^{-i2gt}] \tag{7}$$

$$m(t) = \frac{1}{\sqrt{2}} [A_1(t)e^{i2gt} + iA_2(t)e^{-i2gt}] \tag{8}$$

where  $A_1(t)$  and  $A_2(t)$  are boson operators that satisfy the usual bosonic commutation relations  $[A_1, A_1^\dagger] = [A_2, A_2^\dagger] = 1, [A_1, A_2] = [A_1, A_2^\dagger] = 0$ . Next, we need to substitute straightforwardly Equations (7) and (8) into Equation (6) and employ the RWA, i.e., drop the high-frequency fast oscillation term. Thus, the effective Hamiltonian can be written as

$$H_{eff} = \left(\omega + \frac{K}{4}\right) (A_1^\dagger A_1 + A_2^\dagger A_2) + g(A_1^\dagger A_1 - A_2^\dagger A_2) + \frac{K}{4} (A_1^\dagger A_1 A_1^\dagger A_1 + A_2^\dagger A_2 A_2^\dagger A_2 + 4A_1^\dagger A_1 A_2^\dagger A_2) \tag{9}$$

where  $\omega = (\omega_c + \omega_m)/2$ . For the purpose of simplifying quantum dynamics, let us recur to the Heisenberg equations with respect to  $A_1(t)$  and  $A_2(t)$  as follows

$$i \frac{dA_1(t)}{dt} = (\Omega_1 + 2g)A_1(t) \tag{10}$$

$$i \frac{dA_2(t)}{dt} = (\Omega_2 - 2g)A_2(t) \tag{11}$$

where  $\Omega_1 = \omega + g + \frac{K}{2}(1 + n_{A_1} + 3n_{A_2})$ ,  $\Omega_2 = \omega - g + \frac{K}{2}(1 + n_{A_2} + 3n_{A_1})$ , and  $n_{A_1} = A_1^\dagger(t)A_1(t) = A_1^\dagger(0)A_1(0)$  equivalently for  $n_{A_2}$ . Equations (7)–(11) yield the following expressions

$$a(t) = \frac{1}{\sqrt{2}} [e^{-i\Omega_1 t} A_1(0) - ie^{-i\Omega_2 t} A_2(0)] \tag{12}$$

$$m(t) = \frac{1}{\sqrt{2}} [e^{-i\Omega_1 t} A_1(0) + ie^{-i\Omega_2 t} A_2(0)] \tag{13}$$

For the sake of the subsequent analysis, we adopt the product state of the Glauber coherent state as the initial state in the whole system, i.e.,  $|\alpha_a, \alpha_m\rangle = |\alpha_a\rangle |\alpha_m\rangle$ ; it can also be written as  $|\beta_{A_1} | \beta_{A_2}\rangle = \left| \frac{\alpha_a + \alpha_m}{\sqrt{2}} \right\rangle \left| i \frac{\alpha_a - \alpha_m}{\sqrt{2}} \right\rangle$ . In the following, we will use these initial states to analyze the nonclassical properties of magnons due to Kerr-nonlinearity.

### 3. Kerr-Nonlinearity Trigger Nonclassical Properties

I. *Negativity value of Wigner function.* The Wigner function [43–45] has turned out to be remarkably useful in quantum optics, particularly in the characterization and visualization of nonclassical fields. The Wigner function was first introduced by Wigner in 1932 to the calculate quantum correction to a classic distribution function of a quantum-mechanical

system [45]. The Wigner function is a real function with a quasiprobability distribution property, invariance of coordinate and momentum exchange, and it can take positive values, which can be analogous to the distribution of the Hamiltonian system in classical statistical mechanics. However, the Wigner function can also take negative values, where the occurrence of negative values is not analogical, which is an important manifestation of nonclassical characteristics. Moreover, the Wigner function does not represent the joint measurement distribution of coordinates and momentum of particles in real phase space; that is, it does not describe the probability distribution of coordinates and momentum of particles at the same time. When the Wigner function presents a negative value, it can clearly reflect the nonclassical property of quantum states. The quantum interference structure of the Wigner function directly reflects the nonclassical characteristics of quantum superposition states. Therefore, the negative part of the Wigner function of a specific quantum state can be used as a symbol of nonclassical behavior to describe the quantum interference effect in a concise and vivid way.

We then investigated the presence of the negative value for the Wigner function using the definition given by [43–45]

$$W(\alpha) = \frac{2}{\pi} \text{tr} [D^\dagger(\alpha)\rho_m D(\alpha)(-1)^{m^\dagger m}] \tag{14}$$

where  $\alpha$  is a complex variable,  $\rho_m = |\alpha_m\rangle\langle\alpha_m|$ , and  $D(\alpha) = e^{(\alpha m^\dagger - \alpha^* m)}$  is the displacement operator for Kittel mode  $m$ .

The outcome of the investigation is plotted in Figure 1, which clearly shows the existence of the negative value for the Wigner function when the initial states are ordinary Glauber coherent states. As observed in Figure 1(a–d), the nonlinear effect caused by the Kerr interaction makes the Wigner function of the coherent state negative in some regions of the phase space, thus indicating that the quantum state at this time is a nonclassical state. For the fixed parameter set, the negative volume of the Wigner function may increase, and the nonclassicality of the magnons' quantum state may change sharply when the time  $t$  rises.

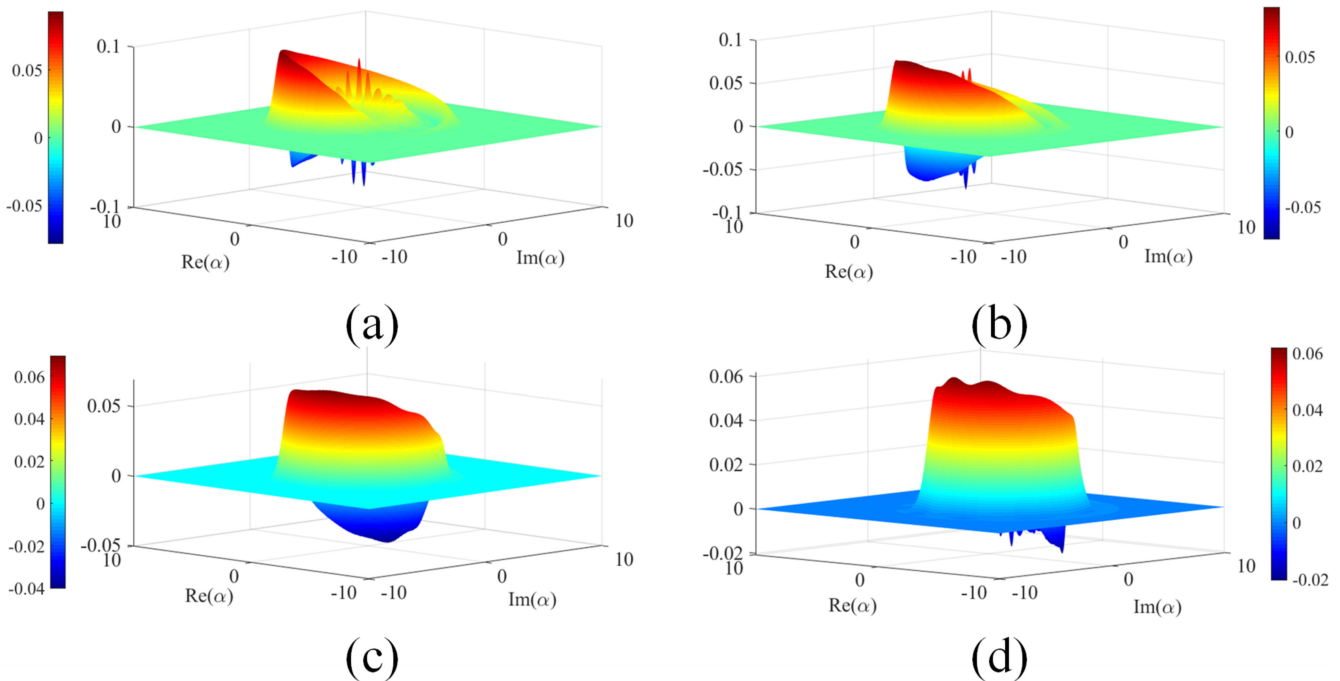


**Figure 1.** The Wigner function  $W(\alpha)$  as a function of  $\text{Re}(\alpha)$  and  $\text{Im}(\alpha)$ , where  $\alpha_a = 4$ ,  $\alpha_m = 2$ ,  $K/\omega = 0.005$  and  $g = 10K$ . (a)  $t = 65$ ; (b)  $t = 70$ ; (c)  $t = 75$ ; (d)  $t = 80$ .

II. *Squeezing effect.* In quantum theory, the squeezed effect is an important nonclassical phenomenon that is peculiar to the quantum field. The squeezed state reflects the nonclassical characteristics of the bose field by means of a noise level that is even lower than that of the coherent state light field (laser field); that is, the noise fluctuation of an orthogonal phase component in the squeezed light is lower than that of the corresponding orthogonal phase component in the laser field. Therefore, in practical applications, if this component is used to transmit information, the signal-to-noise ratio can be higher than that of the coherent state light field, which has a broad application prospect in optical communication, weak signal detection and quantum nondestructive measurement.

In order to attain the squeezing effect, which delineates the nonclassical property of a boson field in the context of the fluctuations in the quadratures  $X_{1m}$  and  $X_{2m}$  of the field, we have the quadrature components of the magnon defined as [45–47]

$$X_1(t) = \frac{1}{2} [m(t) + m^\dagger(t)], X_2(t) = \frac{1}{2i} [m(t) - m^\dagger(t)] \tag{15}$$

Resorting to Ref. [46], we attain the squeezing coefficients

$$S_{im}(t) = \frac{\langle (\Delta X_i(t))^2 \rangle - \frac{1}{2} |\langle [X_1(t), X_2(t)] \rangle|^2}{\frac{1}{2} |\langle [X_1(t), X_2(t)] \rangle|}, i = 1, 2. \tag{16}$$

Substituting Equation (15) into Equation (16), one then straightforwardly obtains

$$S_{1m}(t) = 2\langle m^\dagger(t)m(t) \rangle + 2\text{Re}\langle m^2(t) \rangle - 4[\text{Re}\langle m(t) \rangle]^2 \tag{17}$$

$$S_{2m}(t) = 2\langle m^\dagger(t)m(t) \rangle - 2\text{Re}\langle m^2(t) \rangle - 4[\text{Im}\langle m(t) \rangle]^2 \tag{18}$$

It is evident that when  $t = 0$ , one clearly observes  $S_{im}(t) = 0$ , which indicates that there is no orthogonal squeezed phenomenon, since nonlinear photon-magnon interactions are not introduced. For the case of  $S_{im}(t) < 0$ , it implies that the quadrature component of magnon  $X_{im}$  has been squeezed. In order to show this more clearly, we have drawn a three-dimensional display by choosing  $g = 0.3$ ,  $\alpha_a = 4$  and  $\alpha_m = 2$  in Figure 2. When taking into account the ordinary Glauber coherent state as the initial input field state, we find that the output state of the magnon still displays a periodic orthogonal squeezed behavior with the evolution of time  $t$ , as shown in Figure 2a,b. In this sense, we see that the squeezing effect can be revealed by calculating either the  $S_1(t)$  or  $S_2(t)$  of the  $X_{im}$  component, and one of the two squeeze coefficients  $S_1(t)$  and  $S_2(t)$  always preserves a negative value. As a result, the magnon squeezing behavior exists all the time; it should be mentioned that each has a periodic oscillatory behavior. Simultaneously, as the Kerr coefficient rises, the degree of squeezing is also enhanced. For a fixed time  $t$ , the degree of squeezing may increase rapidly, and the fluctuations in the quadrature  $S_{im}(t)$  of the magnons may change sharply by boosting the Kerr-nonlinearity strength. Therefore, the degree of the squeezing can be manipulated by selecting a suitable nonlinear strength  $K$ .

III. *Antibunching phenomenon.* The antibunching effect is a remarkable manifestation of nonclassicality. By using the second-order correlation function concept, we can quickly and efficiently identify different quantum statistical behaviors. According to quantum statistical methods,  $g^{(2)}(0) = 1$  implies that magnons are randomly distributed, and we cannot seek out the orientation of a single magnon.  $g^{(2)}(0) > 1$  indicates that magnons are inclined to come in flocks and tend to stay in the same place.  $g^{(2)}(0) < 1$  means that magnons do not like to be together and tend to separate or emerge in different places. In other words,  $g_2(0)$  can reflect the repulsive property or attractive features of two magnons. The second-order correlation function  $g^{(2)}(0)$  for a single-mode field is defined as [48–50]

$$g^{(2)}(0) = \frac{\langle m^\dagger(t)m^\dagger(t)m(t)m(t) \rangle}{\langle m^\dagger(t)m(t) \rangle^2} \tag{19}$$

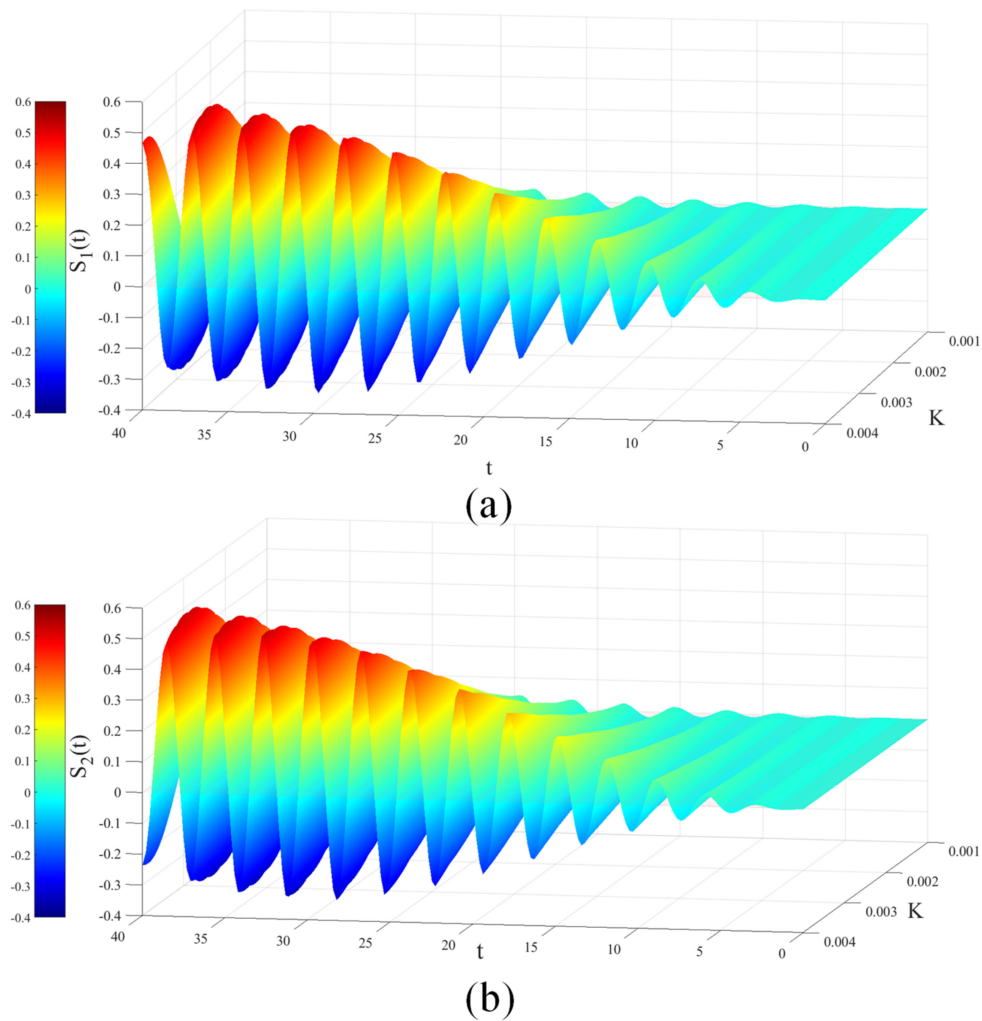


**Figure 2.** The squeezing coefficients  $S_i(t)$  as a function of  $K$  and  $t$ , where  $K$  is dimensionless in units of  $\omega$ ,  $g = 10K$ ,  $\alpha_a = 4$  and  $\alpha_m = 2$ . (a)  $S_1(t) = S_{1m}(t)/|\alpha_a|^2$ , (b)  $S_2(t) = S_{2m}(t)/|\alpha_a|^2$ .

In order to clearly see that the Kerr strength coefficient affects the quantum statistical properties of the single-mode magnon coherent state, we have carried out a direct numerical calculation of  $g^{(2)}(0)$  for a single-mode field with respect to the Kerr strength  $K$  and dimensionless time  $t$ . As shown in Figure 3, we can clearly see the bunching phenomena and the fact that the magnon obeys the super-Poissonian quantum statistics discipline when the Kerr coefficient is smaller than 0.0033. When  $K > 0.0037$ , we can obviously observe that the magnon exhibits an antibunching effect that occupies a major area in Figure 3. In the cross regime of  $0.0033 < K < 0.0037$ , the second-order correlation function of the magnon appears more complex when the Kerr strength  $K$  varies. It is easy to see that, for a single-mode field,  $g^{(2)}(0)$  may decline rapidly when the Kerr-nonlinearity increases. For the sake of confirming this issue, we have plotted  $g^{(2)}(0)$  as a function of the Kerr strength  $K$  with  $t = 9$  and  $t = 10$ , as shown in Figure 4. In order to see this clearly, we draw an auxiliary line (corresponding to  $g^{(2)}(0) = 1$ ) and also mark the transition point position ( $K = K_t \approx 0.00332$  and  $0.00369$ ). In the range  $0.003 < K < K_t$ , the second-order correlation function is bigger than 1; however,  $g^{(2)}(0)$  of the magnon in the range  $K_t < K < 0.006$  is less than 1. Obviously, the magnon number distribution is a Poisson distribution at the transition point  $K_t$ . This implies that the statistical properties of the magnon can be controlled by varying the Kerr-nonlinearity intensity in the photon-magnon system.

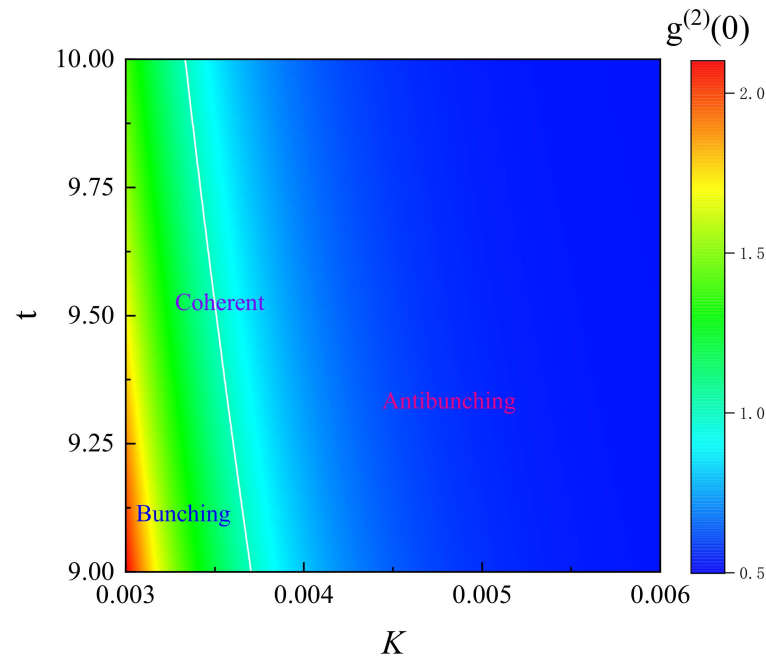


**Figure 3.** The second-order correlation function as a function of  $t$  and  $K$ , where  $K$  is dimensionless in units of  $\omega$ ,  $\alpha_a = 10$ ,  $g = 10K$  and  $\alpha_m = 0.5$ .

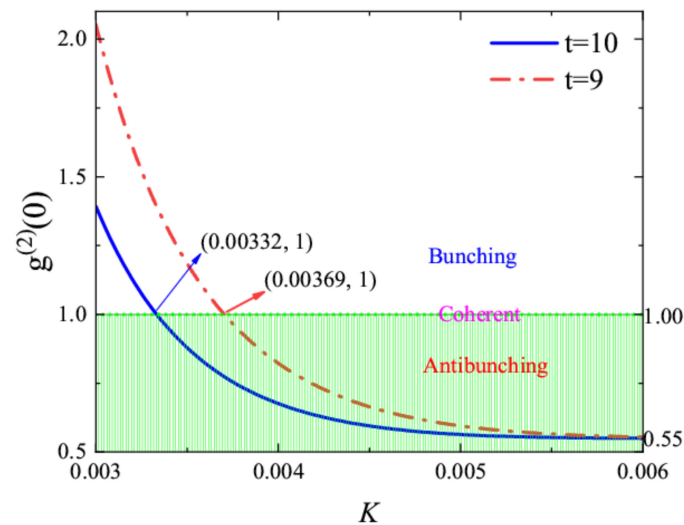


**Figure 4.** The second-order correlation function as a function of  $K$ , where  $K$  is dimensionless in units of  $\omega$ ,  $\alpha_a = 10$ ,  $g = 10K$  and  $\alpha_m = 0.5$ .

**IV. Field nonclassicality.** Similar to the light field, the magnon field is also one of the very important bose fields. The nonclassical states of these bose fields play an increasingly important role as a tool for exploring fundamental quantum theory and quantum technologies. Generally speaking, the nonclassical behavior of the bose field includes squeezing, antibunching, sub-Poissonian statistics, particles' number distribution and so on. The nonclassical nature of describing and quantifying quantum states is a central problem in quantum optics. At present, there are various criteria for detecting nonclassicality and several important nonclassical measures to distinguish nonclassical behavior. However, nonclassical ordering may be inconsistent under different metrics. Due to the complex and subtle characteristics of nonclassicality quantification, these nonclassicality quantification methods have different advantages and disadvantages, and their scope of application is also sharply distinct. As a consequence, it is impossible to obtain a universal measure that is applicable to all targets; that is to say, the above nonclassical measures cannot charac-

terize all aspects of field nonclassicality either. For the sake of exploring the dynamics of the bose field from as many angles as possible to obtain a more complete picture of the dynamics, it is necessary to seek new nonclassical measures based on different perspectives. Fortunately, by resorting to the concept of generalized Wigner–Yanase skew information, the nonclassicality of the field is a nicely effective way to measure the nonclassical property of magnons. According to references [51,52], its definition can be written as

$$N(\rho) = \frac{1}{2} + \text{tr}(\rho m^\dagger(t)m(t)) - \text{tr}(\sqrt{\rho}m^\dagger(t)\sqrt{\rho}m(t)) \tag{20}$$

Here, it is necessary to provide a brief description of field nonclassicality. As everyone knows, the Glauber coherent state  $|\alpha\rangle$  appears to be the closest to the classical behavior of a bose field, and the field nonclassicality of the coherent state is  $1/2$ . In other words, if a state is a pure single-mode quantum state, this pure quantum state’s minimum value of field nonclassicality is  $N(\rho) = 1/2$ . A natural result is that field nonclassicity  $N(\rho) \leq 1/2$  for any single-mode classical state, and we can draw the small conclusion that the quantum state is nonclassical when  $N(\rho) > 1/2$ . Taking the dimensionless time  $t$  and Kerr coefficient  $K$  into account, we draw Figure 5 to observe the quantum dynamics of the field nonclassicality. In Figure 5, we can discover that it can exhibit field nonclassicality in most cases. Simultaneously, from the phase diagram, the nonclassical properties of the magnon show a quasiperiodic variation with time and the Kerr coefficients: for a fixed time, the nonclassical properties increase rapidly as the Kerr coefficients become larger. In other words, the increase in time seems to relax the requirement for the Kerr coefficient. It is worth mentioning that we have no choice of  $t < 20$ ; this is because the Kerr interactions do not accumulate enough, and significant changes will not happen.

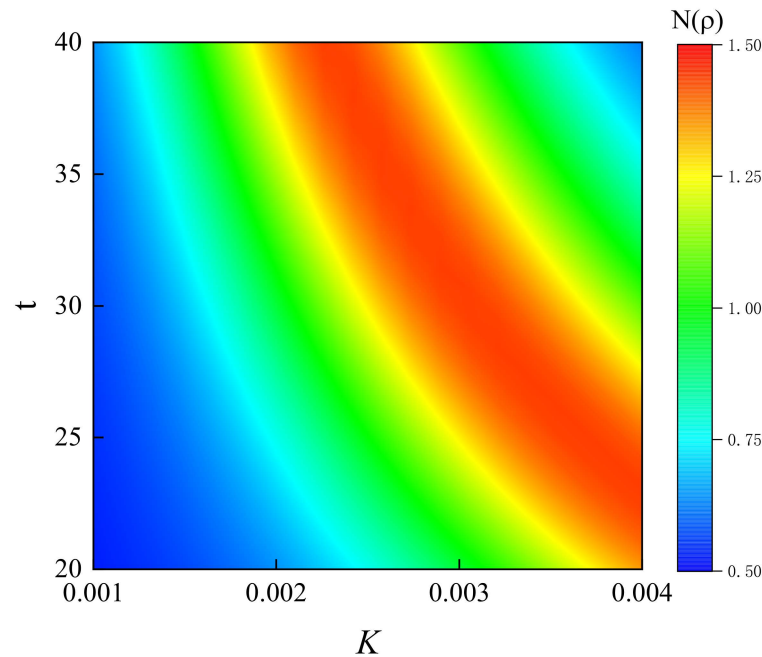


**Figure 5.** Field nonclassicality  $N(\rho)$  as a function of  $t$ .  $K$  is dimensionless in units of  $\omega$ ,  $g = 10K$ ,  $\alpha_a = 4$  and  $\alpha_m = 2$ .

**4. Conclusions**

In conclusion, we have investigated a hybrid system consisting of a YIG sphere and a three-dimensional rectangular microwave cavity, where the two subsystems are coupled by the fundamental mode magnetic field in the microwave cavity. We diagonalized the Hamiltonian of the photon-magnon system with an ingenious transformation. More interestingly, by using the Wigner function, quadrature squeezing operator, second-order correlation function and field nonclassicality, we showed the Kerr-nonlinearity-triggered

nonclassicality of magnons in a photon-magnon coupling system. It has been found that the degree of nonclassicality can be manipulated by adjusting the Kerr nonlinear strength.

**Author Contributions:** Conceptualization, S.T.; methodology, S.T.; software, X.J.; validation, X.J. and S.T.; formal analysis, S.T.; investigation, S.T. and X.J.; resources, S.T.; data curation, X.J.; writing—original draft preparation, X.J.; writing—review and editing, S.T. and S.L.; supervision, S.T. and S.L.; project administration, S.T.; funding acquisition, S.T. All authors have read and agreed to the published version of the manuscript.

**Funding:** This work is supported by the Hunan Provincial Natural Science Foundation of China under Grant Nos. 2020JJ4146 and 2020JJ4002, the Open fund project of the Key Laboratory of Optoelectronic Control and Detection Technology of University of Hunan Province under Grant No. PC20K02, the open fund project of the Key Laboratory of Low-Dimensional Quantum Structures and Quantum Control of Ministry of Education under Grant No. QSQC1907.

**Institutional Review Board Statement:** Not applicable.

**Informed Consent Statement:** Not applicable.

**Data Availability Statement:** Not applicable.

**Conflicts of Interest:** The authors declare no conflict of interest.

## References

1. Xiang, Z.L.; Ashhab, S.; You, J.Q. Hybrid quantum circuits: Superconducting circuits interacting with other quantum systems. *Rev. Mod. Phys.* **2013**, *85*, 623. [[CrossRef](#)]
2. Kurizki, G.; Bertet, P.; Kubo, Y. Quantum technologies with hybrid systems. *Proc. Natl. Acad. Sci. USA* **2015**, *112*, 3866–3873. [[CrossRef](#)] [[PubMed](#)]
3. Soykal, Ö.O.; Flatté, M.E. Strong field interactions between a nanomagnet and a photonic cavity. *Phys. Rev. Lett.* **2010**, *104*, 077202. [[CrossRef](#)] [[PubMed](#)]
4. Soykal, Ö.O.; Flatté, M.E. Size dependence of strong coupling between nanomagnets and photonic cavities. *Phys. Rev. B* **2010**, *82*, 104413. [[CrossRef](#)]
5. Huebl, H.; Zollitsch, C.W.; Lotze, J. High cooperativity in coupled microwave resonator ferrimagnetic insulator hybrids. *Phys. Rev. Lett.* **2013**, *111*, 127003. [[CrossRef](#)]
6. Zhang, D.; Wang, X.M.; Li, T.F. Cavity quantum electrodynamics with ferromagnetic magnons in a small yttrium-iron-garnet sphere. *npj Quantum Inf.* **2015**, *1*, 15014. [[CrossRef](#)]
7. Cherepanov, V.; Kolokolov, I.; L'vov, V. The saga of YIG: Spectra, thermodynamics, interaction and relaxation of magnons in a complex magnet. *Phys. Rep.* **1993**, *229*, 81–144. [[CrossRef](#)]
8. Princep, A.J.; Ewings, R.A.; Ward, S. The Final Chapter In The Saga Of YIG. *arXiv* **2017**, arXiv:1705.06594.
9. Goryachev, M.; Farr, W.G.; Creedon, D.L. High-cooperativity cavity QED with magnons at microwave frequencies. *Phys. Rev. A* **2014**, *2*, 054002. [[CrossRef](#)]
10. Cao, Y.; Yan, P.; Huebl, H. Exchange magnon-polaritons in microwave cavities. *Phys. Rev. B* **2015**, *91*, 094423. [[CrossRef](#)]
11. Yao, B.M.; Gui, Y.S.; Xiao, Y. Theory and experiment on cavity magnon-polariton in the one-dimensional configuration. *Phys. Rev. B* **2015**, *92*, 184407. [[CrossRef](#)]
12. Hyde, P.; Bai, L.; Harder, M. Linking magnon-cavity strong coupling to magnon-polaritons through effective permeability. *Phys. Rev. B* **2017**, *95*, 094416. [[CrossRef](#)]
13. Hisatomi, R.; Osada, A.; Tabuchi, Y. Bidirectional conversion between microwave and light via ferromagnetic magnons. *Phys. Rev. B* **2016**, *93*, 174427. [[CrossRef](#)]
14. Bourhill, J.; Kostylev, N.; Goryachev, M. Ultrahigh cooperativity interactions between magnons and resonant photons in a YIG sphere. *Phys. Rev. B* **2016**, *93*, 144420. [[CrossRef](#)]
15. Grigoryan, V.L.; Shen, K.; Xia, K. Synchronized spin-photon coupling in a microwave cavity. *Phys. Rev. B* **2018**, *98*, 024406. [[CrossRef](#)]
16. Zhang, X.; Zou, C.L.; Zhu, N. Magnon dark modes and gradient memory. *Nat. Commun* **2015**, *6*, 8914. [[CrossRef](#)]
17. Bai, L.; Harder, M.; Chen, Y.P. Spin pumping in electro-dynamically coupled magnon-photon systems. *Phys. Rev. Lett.* **2015**, *114*, 227201. [[CrossRef](#)]
18. Braggio, C.; Carugno, G.; Guarise, M. Optical manipulation of a magnon-photon hybrid system. *Phys. Rev. Lett.* **2017**, *118*, 107205. [[CrossRef](#)]
19. Chen, J.; Liu, C.; Liu, T. Strong interlayer magnon-magnon coupling in magnetic metal-insulator hybrid nanostructures. *Phys. Rev. Lett.* **2018**, *120*, 217202. [[CrossRef](#)]
20. Yao, B.; Gui, Y.S.; Rao, J.W. Cooperative polariton dynamics in feedback-coupled cavities. *Nat. Commun.* **2017**, *8*, 1437. [[CrossRef](#)]

21. Tabuchi, Y.; Ishino, S.; Noguchi, A. Coherent coupling between a ferromagnetic magnon and a superconducting qubit. *Science* **2015**, *349*, 405–408. [[CrossRef](#)] [[PubMed](#)]
22. Gao, Y.P.; Cao, C.; Wang, T.J. Cavity-mediated coupling of phonons and magnons. *Phys. Rev. A* **2017**, *96*, 023826. [[CrossRef](#)]
23. Anderson, P.W.; Suhl, H. Instability in the motion of ferromagnets at high microwave power levels. *Phys. Rev.* **1955**, *100*, 1788. [[CrossRef](#)]
24. Rezende, S.M.; de Aguiar, F.M. Spin-wave instabilities, auto-oscillations, and chaos in yttrium-iron-garnet. *Proc. IEEE* **1990**, *78*, 893–908. [[CrossRef](#)]
25. Bi, M.X.; Yan, X.H.; Zhang, Y. Tristability of cavity magnon polaritons. *Phys. Rev. B* **2021**, *103*, 104411. [[CrossRef](#)]
26. Bi, M.X.; Yan, X.H.; Xiao, Y. Magnon dark mode in a strong driving microwave cavity. *J. Appl. Phys.* **2019**, *126*, 173902. [[CrossRef](#)]
27. Bi, M.X.; Yan, X.H.; Xiao, Y. Sharply vanishing destructive interference induced by magnon Kerr effect in cavity magnon polaritons. *J. Appl. Phys.* **2020**, *127*, 223909. [[CrossRef](#)]
28. Bi, M.X.; Yan, X.H.; Xiao, Y. Manipulation of bistability through the coupling strength in cavity magnon polaritons. *J. Phys. D Appl. Phys.* **2020**, *53*, 345001. [[CrossRef](#)]
29. Blundell, S. *Magnetism in Condensed Matter*; Oxford University Press: Oxford, UK, 2001.
30. Zhang, G.Q.; You, J.Q. Higher-order exceptional point in a cavity magnonics system. *Phys. Rev. B* **2019**, *99*, 054404. [[CrossRef](#)]
31. Xiong, W.; Chen, J.; Fang, B. Coherent perfect absorption in a weakly coupled atom-cavity system. *Phys. Rev. A* **2020**, *101*, 063822. [[CrossRef](#)]
32. Wang, Y.P.; Zhang, G.Q.; Zhang, D. Bistability of cavity magnon polaritons. *Phys. Rev. Lett.* **2018**, *120*, 057202. [[CrossRef](#)]
33. Zhang, G.Q.; Wang, Y.P.; You, J.Q. Theory of the magnon Kerr effect in cavity magnonics. *Sci. China Phys.* **2019**, *62*, 987511. [[CrossRef](#)]
34. Liu, Z.X.; Wang, B.; Xiong, H. Magnon-induced high-order sideband generation. *Opt. Lett.* **2018**, *43*, 3698–3701. [[CrossRef](#)]
35. Liu, Z.X.; You, C.; Wang, B. Phase-mediated magnon chaos-order transition in cavity optomagnonics. *Opt. Lett.* **2019**, *44*, 507–510. [[CrossRef](#)]
36. Zhang, G.Q.; Chen, Z.; Xiong, W. Parity-symmetry-breaking quantum phase transition via parametric drive in a cavity magnonic system. *Phys. Rev. B* **2021**, *104*, 064423. [[CrossRef](#)]
37. Xiong, W.; Tian, M.; Zhang, G.Q.; You, J.Q. Strong long-range spin-spin coupling via a Kerr magnon interface. *Phys. Rev. B* **2022**, *105*, 245310. [[CrossRef](#)]
38. Wang, Y.M.; Xiong, W.; Xu, Z.Y.; Zhang, G.Q.; You, J.Q. Dissipation-induced nonreciprocal magnon blockade in a magnon-based hybrid system. *Sci. China Phys. Mech. Astron.* **2022**, *65*, 260314. [[CrossRef](#)]
39. Wang, Y.P.; Zhang, G.Q.; Zhang, D. Magnon Kerr effect in a strongly coupled cavity-magnon system. *Phys. Rev. B* **2016**, *94*, 224410. [[CrossRef](#)]
40. Kuang, L.M.; Ouyang, Z.W. Macroscopic quantum self-trapping and atomic tunneling in two-species Bose-Einstein condensates. *Phys. Rev. A* **2000**, *61*, 023604. [[CrossRef](#)]
41. Jing, H.; Chen, J.L.; Ge, M.L. Squeezing effects of an atom laser: Beyond the linear model. *Phys. Rev. A* **2001**, *65*, 015601. [[CrossRef](#)]
42. Haghshenasfarda, Z.; Cottamb, M.G. Sub-Poissonian statistics and squeezing of magnons due to the Kerr effect in a hybrid coupled cavity-magnon system. *J. Appl. Phys.* **2020**, *128*, 033901. [[CrossRef](#)]
43. Schleich, W.P. *Quantum Optics in Phase Space*; John Wiley & Sons: New York, NY, USA, 2011.
44. Wigner, E. On the quantum correction for thermodynamic equilibrium. *Phys. Rev.* **1932**, *40*, 749. [[CrossRef](#)]
45. Walls, D.F.; Milburn, G.J. *Quantum Optics*; Springer: Berlin/Heidelberg, Germany, 1994.
46. Buzek, V.; Vidiella-Barranco, A.; Knight, P.L. Superpositions of coherent states: Squeezing and dissipation. *Phys. Rev. A* **1992**, *45*, 6570–6585. [[CrossRef](#)]
47. Naikoo, J.; Thapliyal, K.; Pathak, A. Probing nonclassicality in an optically driven cavity with two atomic ensembles. *Phys. Rev. A* **2018**, *97*, 063840. [[CrossRef](#)]
48. Xie, J.; Ma, S.; Li, F. Quantum-interference-enhanced magnon blockade in an yttrium-iron-garnet sphere coupled to superconducting circuits. *Phys. Rev. A* **2020**, *101*, 042331. [[CrossRef](#)]
49. Liu, Z.X.; Xiong, H.; Wu, M.Y. Absorption of magnons in dispersively coupled hybrid quantum systems. *Phys. Rev. A* **2021**, *103*, 063702. [[CrossRef](#)]
50. Wang, F.; Gou, C.; Xu, J. Hybrid magnon-atom entanglement and magnon blockade via quantum interference. *Phys. Rev. A* **2022**, *106*, 013705. [[CrossRef](#)]
51. Luo, S.; Zhang, Y. Quantifying nonclassicality via Wigner-Yanase skew information. *Phys. Rev. A* **2019**, *100*, 032116. [[CrossRef](#)]
52. Fu, S.; Luo, S.; Zhang, Y. Dynamics of field nonclassicality in the Jaynes-Cummings model. *Quantum Inf. Process.* **2021**, *20*, 88. [[CrossRef](#)]